

Hybrid Model Predictive Flight Mode Conversion Control of Unmanned Quad-TiltRotors

Christos Papachristos¹, Kostas Alexis² and Anthony Tzes³

Abstract—In this paper the autonomous flight mode conversion control scheme for a Quad-TiltRotor Unmanned Aerial Vehicle is presented. This convertible UAV type has the capability for flying both as a helicopter as well as a fixed-wing aircraft type, by adjusting the orientation of its tilt-enabled rotors. Thus, a platform combining the operational advantages of two commonly distinct aircraft types is formed. However, its autonomous mid-flight conversion is an issue of increased complexity. The approach presented is based on an innovative control scheme, developed based on hybrid systems theory. Particularly, a piecewise affine modeling approximation of the complete nonlinear dynamics is derived and serves as the model for control over which a hybrid predictive controller that provides global stabilization, optimality and constraints satisfaction is computed. The effectiveness of the proposed control scheme in handling the mode conversion from helicopter to fixed-wing (and conversely) is demonstrated via a series of simulation studies. The proposed control scheme exceeds the functionality of the aforementioned flight-mode conversion and is also able to handle the transition to intermediate flight-modes with rotors slightly tilted forward in order to provide a forward force component while flying in close to helicopter-mode.

I. INTRODUCTION

The area of Unmanned Aerial Vehicles (UAVs) has proven to be a pioneering research field with a wide variety of civilian applications. Due to the reduced time and cost requirements in the platform development and testing processes, numerous innovative UAV platforms are constantly emerging; however certain applications, characterized by increased mission complexity, and their respective research and design goals still remain unaddressed.

Operational scenarios including search and assistance provision missions, ongoing natural disaster phenomena monitoring, border-line or power-line autonomous inspection and a multitude of similar missions, require: a) close-range inspection of small-scale areas, combined with b) high-speed surveillance of wide areas. This raises the demand for specialized UAV platforms, capable of: a) efficient and prolonged endurance flight, and b) navigating into constrained areas, while c) maintaining full operational autonomy.

In this paper, a rotor-tilting convertible UAV platform, namely the Quad-TiltRotor concept shown in Figure 1, is considered. The proposed platform is capable of adjusting the orientation of its rotors concurrently with its wings' angles of attack, by rotating them relative to the fuselage axes. This

enables two discrete modes of operation: *i*) a helicopter-like Vertical Take-Off and Landing (VTOL) mode, with its rotors facing upwards, and *ii*) a fixed-wing aircraft-like longitudinal flight mode, with its rotors tilted forward.

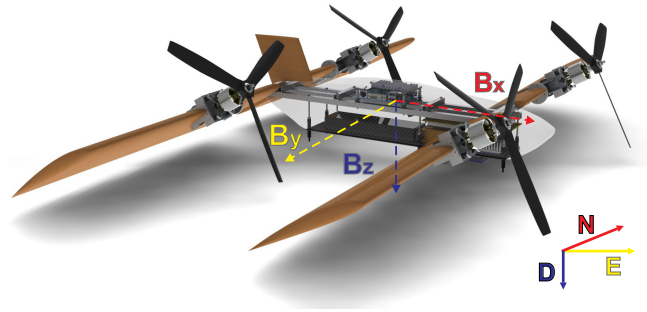


Fig. 1. The Quad-TiltRotor concept platform

In order to achieve a fully autonomous convertible system, it is required that the UAV be capable of achieving mid-flight, helicopter-to-fixed wing (and conversely) mode conversion maneuvers, based on a reliable and non human-aided control scheme. The challenge summarized by this necessity is the main focus of the work presented: Initially, a model of the full-flight envelope nonlinear dynamics is deduced and analytically presented. Following this, a novel hybrid model predictive control (hybrid-MPC) [1, 2] strategy that relies on a piecewise affine modeling approximation of the complete nonlinear dynamics is presented. The proposed controller is capable of ensuring global stability of the hybrid system and response optimality, while respecting the modeled input and state constraints. The implemented Piecewise Affine (PWA) approximation of the nonlinear dynamics can be adjusted for higher or lower fidelity, based on the confidence of the aerodynamic parameters and the available computational power. Eventually, the hybrid-MPC efficiently achieves execution of both types of flight mode conversion maneuvers. Additionally, it can benefit from advantageous characteristics of intermediate flight-mode regions, such as the mostly-helicopter mode with the rotors tilted forward thus enabling the UAV's fast forward flight, and effectively achieve more aggressive control maneuvers.

The article is structured as follows: In Section II the Quad-TiltRotor's nonlinear model is described. In Section III the system modeling for control purposes is presented, and in Section IV the implemented control scheme is analyzed. In Section V a series of simulation studies of the proposed scheme are presented. The article is concluded in Section VI.

¹C. Papachristos and ³A. Tzes are with the Electrical and Computer Engineering Department, University of Patras, Greece papachric(tzes)@ece.upatras.gr

²K. Alexis is with the Swiss Federal Institute of Technology (ETHZ), ASL, Tannenstrasse 3, 8092 Zuerich konstantinos.alexis@mavt.ethz.ch

II. SYSTEM MODELING

The Quad-TiltRotor's operating principles in the helicopter-like hovering mode, the fixed-wing longitudinal flight mode and the intermediate flight mode conversion phase are depicted in Figure 2. The Body-Fixed coordinates Frame (BFF) $\mathbf{B} = \{B_x, B_y, B_z\}$ and the North-East-Down (NED) [3] Local Tangential coordinates Plane (LTP) $\mathbf{E} = \{N, E, D\}$ are shown in Figure 1.

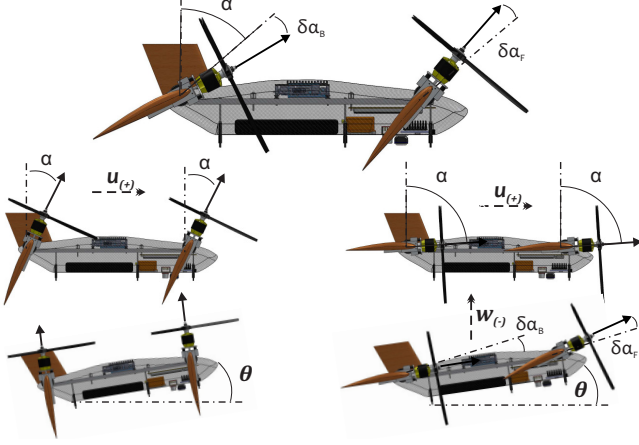


Fig. 2. The Quad-TiltRotor's operating principles

Let $\Omega = \{p, q, r\}$ be the BFF rotational rates vector and $\Theta = \{\phi, \theta, \psi\}$ the LTP rotation angles vector. Also let $\mathbf{U} = \{u, v, w\}$ be the BFF velocity vector and $\mathbf{X}^W = \{x^W, y^W, z^W\}$ the LTP position vector. Via the Newton-Euler formulation the system's nonlinear dynamics are modeled as:

$$\begin{aligned} \mathbf{F}^B &= m\dot{\mathbf{U}} + \Omega \times (m\mathbf{U}) & \mathbf{M}^B &= \mathbf{I}\dot{\Omega} + \Omega \times (\mathbf{I}\Omega) \\ \dot{\mathbf{X}}^W &= \mathbf{R}^{B \rightarrow W} \mathbf{U} & \dot{\Theta} &= \mathbf{J}^{B \rightarrow W} \Omega, \end{aligned} \quad (1)$$

where $\mathbf{F}^B = \{F_x, F_y, F_z\}$ the BFF total Force vector, $\mathbf{M}^B = \{M_x, M_y, M_z\}$ the BFF total Moment vector, m the mass and \mathbf{I} the moment of inertia matrix. Also, $\mathbf{R}^{B \rightarrow W}$ is the BFF \rightarrow LTP translational velocities transformation matrix and $\mathbf{J}^{B \rightarrow W}$ the Tait-Bryan rotational rates transformation matrix [4].

For the purposes of this paper, the control of the pitch $\{q, \theta\}$, the altitude $\{w, z^W\}$ and the forward flight $\{u, x^W\}$ subsystems will be analyzed, as they adequately capture the majority of the phenomena during a flight mode transition maneuver, while the reference model derived, is utilized in simulation studies verifying the effectiveness of the proposed flight mode transition control scheme.

In the helicopter-like VTOL mode, the pitch is controlled via the differential thrusting of the front and back rotors, the altitude vertical motion is controlled via the total thrust produced by the 4 rotors and the longitudinal forward motion is controlled via vectoring/projection of the main rotors' thrust vectors, by equally tilting them by an angle α .

In the fixed-wing mode, the pitch is controlled by differentially tilting the front and back rotor/wing system by angles $\{\delta\alpha_F, \delta\alpha_B\}$, thus achieving: a) differential vectoring of the front and back rotors' thrust, and b) differential lift forces

produced by the front and back wing aerodynamic surfaces. The altitude and forward flight motions are controlled by adjusting a) the common rotor/wing angles α and b) the thrust produced by the rotors. Via combining: a) rotor thrust control, and b) the collective lift produced by the front and back wings, varying $\{F_x, F_z\}$ components are achieved.

During flight mode transition, the conversion process as well as the stability and response optimality of the UAV are handled by a hybrid control scheme, more extensively described in Sections III, IV.

A. RIGID BODY MODEL

The proposed Quad-TiltRotor concept platform was designed in detail and its parameters optimized making use of 3D CAD software. Let $j \rightarrow [F, B]$ mark the set of the two front and back rotors with respect to the B_x positive axis and let α_j be the angle of the j -th rotor-set with respect to the B_z axis. Also let d_{j_p} be the BFF- p -direction component of the geometric distance from the Center of Mass (COM) to the j -th rotor-set tilt axis, and h_j the distance of the j -th rotor-set propeller hub from their tilt axis. Finally, let I_{xx}, I_{yy}, I_{zz} be the rigid body moments of inertia around the BFF axes. The dominant model parameters are presented in Table I.

TABLE I
QUAD-TILTROTOR SYSTEM PARAMETERS

Property	Value	Units	Property	Value	Units
d_{F_x}, d_{B_x}	0.20	m	I_{xx}	0.063428242	kg-m ²
d_{F_y}, d_{B_y}	0.25	m	I_{yy}	0.038492375	kg-m ²
d_{F_z}, d_{B_z}	0.003	m	I_{zz}	0.085204883	kg-m ²
h_F, h_B	0.099	m	m	4.102	kg
$[K_{p_r}, T_{p_r}, T_{d_r}]$	[4 0.19 0.034]		T_{d_r}	0.020	s

The rigid body Forces and Moments are modeled as:

Gravitational Forces: Let $\mathbf{G}^B = (\mathbf{R}^{B \rightarrow W})^{-1} \mathbf{G}^W$ be the BFF-expressed gravity vector, where $\mathbf{G}^W = [0 \ 0 \ mg]^T$, ($g = 9.81 \text{ m/s}^2$) the LTP gravity vector.

Rotor Thrust Forces and Moments:

$$\mathbf{F}_{r,j} = [F_{j_x} \ F_{j_y} \ F_{j_z}]^T = \begin{bmatrix} F_j \sin(\alpha_j) \\ 0 \\ -F_j \cos(\alpha_j) \end{bmatrix} \quad (2)$$

$$F_j = k_T \Omega_j^2,$$

where F_j the j th rotor-set Thrust Force, Ω_j the respective angular speed and $k_T = 4.0789 \cdot 10^{-5} \text{ N/(rad/s)}^2$ a rotor thrust coefficient, experimentally determined. It should be noted that the negative signum in the F_{j_z} component is due to the NED-notation. Also the respective moments,

$$\begin{aligned} \mathbf{M}_{r,j} &= \mathbf{F}_{r,j} \times \mathbf{r}_j \\ \mathbf{r}_j &= [r_{j_x} \ r_{j_y} \ r_{j_z}]^T = \begin{bmatrix} d_{j_x} + h_j \sin(\alpha_j) \\ \pm d_{j_y} \\ -(d_{j_z} + h_j \cos(\alpha_j)) \end{bmatrix}, \end{aligned} \quad (3)$$

where r_{j_p} the j th rotor-set position vector component in the BFF p -direction, from the COM to the propeller hub. Let it be noted that $r_{j_y} = \pm d_{j_y}$ marks the right/left rotor position vector component consisting the j th rotor-set.

Rotor Gyroscopic Moments: The rotating propellers are the subject of a gyroscopic effect while tilting:

$$\mathbf{M}_{G,j} = \mathbf{I}_{r,j}(\dot{\alpha}_j \times \Omega_j), \quad (4)$$

where $\mathbf{I}_{r,j}$ the j th rotor-set inertia and $\dot{\alpha}_j = [0 \ \dot{\alpha}_j \ 0]^T$.

Rotor Drag Moments: The moment exerted on the hub of each rotor during rotation due to the propeller's drag:

$$\mathbf{M}_{D,j} = k_D \Omega_j^2,$$

which for identical rotational speeds in each rotor-set are counter-acting and zeroed-out.

B. AERODYNAMIC MODEL

The standard NACA2411 airfoil was selected for the wing design. Each wing has a total span of $w_l = 1\text{m}$ and constant chord of $w_c = 0.2\text{m}$. The wings are mounted on the rotor-tilting mechanisms such that the airfoil chord line is coincident with the rotor central axis. Thus, the wing rotates along with the rotor for a full 90-degree angle, and the wing angle of attack is equal to the rotor-set angle α_j .

Due to lack of experimental data for the full range of angle of attack α_j and low Reynolds numbers, the XFOIL [5] airfoil analysis software was utilized in obtaining the wing lift coefficients $c_l(u, \alpha_j)$ and drag coefficients $c_d(u, \alpha_j)$. It should be noted that c_l , c_d are also functions of u , as the airfoil aerodynamic analysis of XFOIL is performed for $\alpha_j \rightarrow [0, 90]$ for specific Reynolds numbers, thus producing datasets for a 2-parameter lookup table (Figure 3).

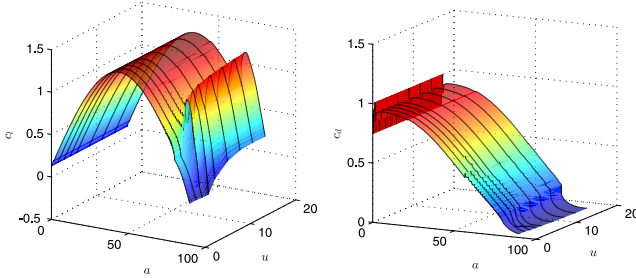


Fig. 3. Lift and Drag Coefficients Interpolated Data Lookup Tables

Wing Forces : Due to the forward longitudinal speed u of the aircraft, the wing aerodynamic surfaces produce forces expressed on the BFF as:

$$\mathbf{F}_{w,j} = [-D(u, \alpha_j) \ 0 \ -L(u, \alpha_j)]^T = \begin{bmatrix} -\frac{1}{2}\rho c_d(u, \alpha_j)Au^2 \\ 0 \\ -\frac{1}{2}\rho c_l(u, \alpha_j)Au^2 \end{bmatrix} \quad (5)$$

$$A = |w_c w_l \sin(\alpha_j)|,$$

where $L(u, \alpha_j)$ the lift force and $D(u, \alpha_j)$ the drag force of the j -th wing for an angle of attack α_j .

Wing Moments : The forces are exerted on the wing Aerodynamic Center (AC), located at approximately $\frac{w_l}{4}$, therefore the j th Moment Origin position vector $\mathbf{r}_{w,j}$ is:

$$\mathbf{M}_{w,j} = \mathbf{F}_{w,j} \times \mathbf{r}_{w,j} \quad (6)$$

$$\mathbf{r}_{w,j} = [r_{w,jx} \ r_{w,jy} \ r_{w,jz}]^T = \begin{bmatrix} d_{jx} \frac{w_l}{4} \sin(\alpha_j) \\ 0 \\ -(d_{jz} - \frac{w_l}{4} \cos(\alpha_j)) \end{bmatrix}.$$

Fuselage Drag Force : The Quad-TiltRotor fuselage drag in forward flight was modeled via the rough approximation:

$$\mathbf{D}_F = [-(p_1 u^2 + p_2 u) \ 0 \ 0]^T, \quad (7)$$

with $p_1 = 0.1$ and $p_2 = 0.5$, such that the drag force exerted at a flight speed of $u = 15\text{m/s}$ is equal to 30N. The nonlinearity of the fuselage drag force relationship is efficiently handled by the conversion hybrid control scheme, as is demonstrated in Section V.

In Figure 4 the equilibrium path ($\mathbf{F}^B = \mathbf{0}$) in the $[\alpha_j, u]$ space for a conversion maneuver is visualized. The blue/red color-graded surface is the fuselage drag force D_F and the light blue/purple color-graded surface represents the forward thrust force $F_x = \sum_{j=F,B} (F_{jx} - D(u, \alpha_j))$ that would be required in order to maintain $F_z = 0$ at that particular $[\alpha_j, u]$ combination. The intersection of the two surfaces $F_x = D_F$ represents the points where the total force \mathbf{F}^B is zero.

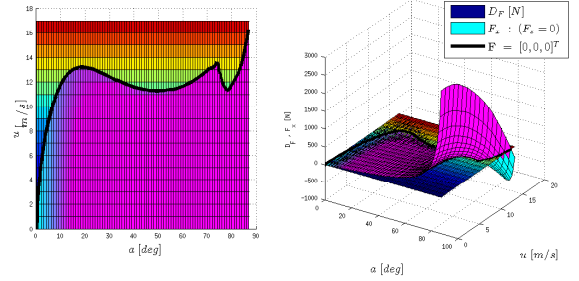


Fig. 4. Equilibrium Path for a Conversion-like Maneuver, $\alpha_j : 0 \rightarrow 90[\text{deg}]$

The fixed-wing mode trim point operating conditions $[\alpha_j^{FW}, u^{FW}]$ and the respective Ω_j^{FW} are calculated from selecting the point at which the wing lift coefficient relationship $c_l(\alpha_j)$ is at its linear lift region. This is adequately achieved at $[\alpha_j^{FW}, u^{FW}] = [86.35 \text{ deg}, 15 \text{ m/s}]$.

C. ACTUATORS MODEL

The model of the actual actuation subsystem of an existing TiltRotor UAV implementation was utilized, which was obtained via an identification procedure as presented in [6]:

$$\frac{\Omega_j(s)}{U_{r,j}(s)} = \frac{K_{P_r}}{(1 + T_{P_r}s)} e^{-T_{d_r}s}, \quad j \rightarrow [F, B] \quad (8)$$

$$\frac{\alpha_j(s)}{U_{s,j}(s)} = e^{-T_{d_s}s}, \quad j \rightarrow [F, B],$$

where $U_{r,j}$ and $U_{s,j}$ marking the rotor and servo control input commands of the j th rotor-set. The identified parameters are presented in Table I.

D. STATE-SPACE REPRESENTATION

From (1) and for

$$\mathbf{F}^B = \sum_{j=F,B} (\mathbf{F}_{r,j} + \mathbf{F}_{w,j}) + \mathbf{D}_F + \mathbf{G}^B$$

$$\mathbf{M}^B = \sum_{j=F,B} (\mathbf{M}_{r,j} + \mathbf{M}_{G,j} + \mathbf{M}_{w,j}),$$

the nonlinear system dynamics model is fully defined. The full state vector is $\mathbf{X}^F = [\Theta \ \Omega \ \mathbf{X}^W \ \mathbf{U} \ \Omega_F \ \Omega_B \ \alpha_F \ \alpha_B]^T$,

however as previously analyzed, for the purposes of control analysis and design of the scheme presented in this paper, the reduced $\mathbf{x} = [\theta \ q \ w \ u \ \alpha]^T$, $\alpha = (\alpha_F + \alpha_B)/2$ and the control inputs $\mathbf{u} = [\Omega_F^d \ \Omega_B^d \ \delta\alpha_F^d \ \delta\alpha_B^d \ \alpha^d]^T$, $\alpha_F^d = \alpha^d + \delta\alpha_F^d$, $\alpha_B^d = \alpha^d + \delta\alpha_B^d$ are utilized. Let the aforementioned subsystem's dynamics be abbreviated into the following nonlinear equation:

$$\dot{\mathbf{x}} = f(\mathbf{x}, \mathbf{u}). \quad (9)$$

III. MODELING FOR CONTROL

As presented in Section II, the dynamics that govern the full flight envelope of a Quad-TiltRotor are highly nonlinear, while the estimation of the aerodynamic parameters within the transition area contains significant uncertainty. This fact poses more challenges towards the need to develop globally stabilizing controllers with optimal responses in order to perform the transition maneuver in a completely autonomous sense. Despite the potential applications of convertible MAVs and the rich field experience with manned or large semi-autonomous Unmanned Tilt-Rotors there is only limited research papers that deal with this problem [7, 8].

Due to the modeling complexity and aerodynamic parameters estimation uncertainty it was thought that a model-based control strategy that relies on the complete non-linear model is not necessarily the proper way to tackle the problem. Within this paper a hybrid control approach that relies on a configurable hybrid modeling approach is proposed. The derived controller can guarantee global stabilization of the hybrid system during the transition between different flight models, while providing response optimality and constraints satisfaction. The derived hybrid control approach relies on a piecewise affine (PWA) approximation of the multi-mode flight envelope. Through such a piecewise representation the designer has the flexibility to increase or decrease the fidelity according to the confidence on the estimated parameters, the desired flying modes and the available computational power. Moreover, through the affine terms, the effect of non-trimmed forces and moments during the transition is taken into account hence providing this crucial information to the control design process.

The derivation of the PWA representations comes directly through the nonlinear dynamics which are linearized over different rotor/servo angles and different forward velocities. These two states govern the transition between the different flight modes. The two main flight modes are the helicopter and fixed-wing mode, while it is thought that flight modes with servo angles close to these two extreme cases can also be useful. For example, a flight mode with the rotors tilted slightly forward is appropriate for fast forward-flight in a close to helicopter flight mode and control methodology. The derivation of the dynamics at each flight mode is achieved through linearization of (9) around a specific mean servo angle $\alpha = (\alpha_F + \alpha_B)/2 = \alpha_k$ and a specific forward velocity $u = u_j$:

$$\dot{\mathbf{x}} = f(\mathbf{x}, \mathbf{u}) \Big|_{\substack{\alpha=\alpha_k \\ u=u_j}} \quad (10)$$

By performing this linearization step for a set of different servo angles and forward velocities, a hybrid model in the form of a PWA representation derived. Within the framework of this paper, the following sets of servo angles and forward velocities were considered:

$$\begin{aligned} \mathbf{S}(\alpha) &= \{0, 15, 30, 45, 60, 75, 86.35\} \text{ (deg)} \\ \mathbf{S}(u) &= \{0, 15\} \text{ (m/s)} \end{aligned} \quad (11)$$

As seen, the minimum required set of different forward velocities corresponding to hovering and trimmed forward flight velocity in fixed-wing mode was utilized while a step of 15 degrees was used for the servo angles. As an exception, the final servo angle is not 90 but 86.35 degrees which corresponds to the fixed-wing mode as explained in Section II. Figure 5 illustrates the selected operating points that form the PWA representation.

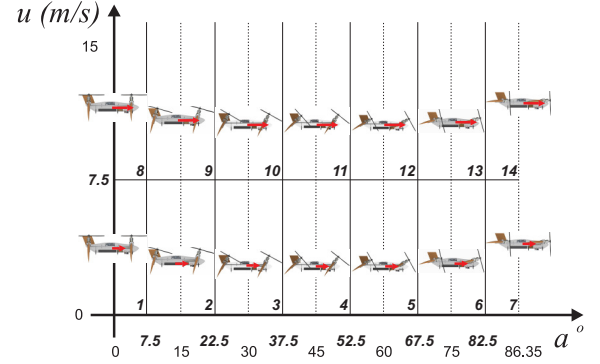


Fig. 5. Visualization of the different modes modeled within the hybrid systems approach. The number at the bottom corner is the index of every PWA system.

Finally, a step of discretization with sampling time $T_s = 0.01$ is performed and the PWA representation takes the following form:

$$\begin{aligned} \mathbf{x}(k+1) &= \mathbf{A}_{i(k)}\mathbf{x}(k) + \mathbf{B}_{i(k)}\mathbf{u}(k) + \mathbf{f}_{i(k)} \\ \mathbf{y}(k) &= \mathbf{C}_{i(k)}\mathbf{x}(k) + \mathbf{D}_{i(k)}\mathbf{u}(k) \end{aligned} \quad (12)$$

where $m \rightarrow f, l$ denotes either the forward motion or the lateral dynamics and $i(k)$ such that:

$$\begin{aligned} \mathbf{H}_{i(k)}\mathbf{x}(k) + \mathbf{J}_{i(k)}\mathbf{u}(k) &\leq \mathbf{K}_{i(k)} \\ \tilde{\mathbf{H}}_{i(k)}\mathbf{x}(k) + \tilde{\mathbf{J}}_{i(k)}\mathbf{u}(k) &< \tilde{\mathbf{K}}_{i(k)} \end{aligned} \quad (13)$$

where $\mathbf{x} \in X \subset \mathbb{R}^n$, $\mathbf{u} \in U \subset \mathbb{R}$, $\mathbf{y} \in Y \subset \mathbb{R}^p$, the matrices $\mathbf{A}_{i(k)}$, $\mathbf{B}_{i(k)}$, $\mathbf{f}_{i(k)}$, $\mathbf{C}_{i(k)}$, $\mathbf{D}_{i(k)}$, $\mathbf{H}_{i(k)}$, $\mathbf{J}_{i(k)}$, $\mathbf{K}_{i(k)}$, $\tilde{\mathbf{H}}_{i(k)}$, $\tilde{\mathbf{J}}_{i(k)}$, $\tilde{\mathbf{K}}_{i(k)}$ are constant and have suitable dimensions, $i(k) = 1, \dots, s$ where $s = n_\alpha \cdot n_u$ is the number of the utilized PWA systems, n_α the number of servo angle points and n_u the number of different forward velocities used for the PWA family. The last matrix inequalities are called guard conditions and govern the switching rule. Note also the presence of the affine term $\mathbf{f}_{i(k)}$ which accounts for the non-trimmed forces and moments in the non-nominal flight modes.

IV. FLIGHT MODE TRANSITION CONTROL

The PWA representation of the Quad-TiltRotor nonlinear dynamics serves as the basis for the synthesis of the proposed flight mode transition controller. Figure 6 presents a block diagram of the hybrid model predictive controller (hybrid MPC) in feedback connection with the aircraft dynamics. The proposed control scheme provides velocity control on w, u and absolute orientation control on θ, q and the rotors tilting α_F, α_B and their mean tilt angle $\alpha = (\alpha_F + \alpha_B)/2$.

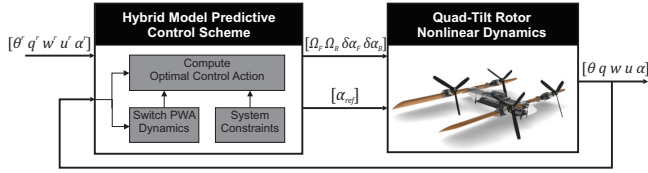


Fig. 6. Block diagram of the proposed hybrid model predictive control approach

As mentioned, the proposed control strategy is able to handle the state and actuation constraints of the system. The following set of hard input and state constraints were modeled and applied during the control derivation process.

$$\begin{bmatrix} \mathbf{I}_{4 \times 4} & \mathbf{0}_{4 \times 4} \\ \mathbf{0}_{4 \times 4} & -\mathbf{I}_{4 \times 4} \end{bmatrix} \begin{bmatrix} \theta \\ q \\ w \\ u \end{bmatrix}^T \leq \begin{bmatrix} 10 \text{deg} \\ 40 \text{deg/s} \\ 1 \text{m/s} \\ 30 \text{m/s} \\ 10 \text{deg} \\ 40 \text{deg/s} \\ 1 \text{m/s} \\ 30 \text{m/s} \end{bmatrix}, \quad \begin{bmatrix} \mathbf{I}_{4 \times 4} & \mathbf{0}_{4 \times 4} \\ \mathbf{0}_{4 \times 4} & -\mathbf{I}_{4 \times 4} \end{bmatrix} \begin{bmatrix} \alpha_F \\ \Omega_B \\ \delta \alpha_F \\ \delta \alpha_B \\ \Omega_F \\ \Omega_B \\ \delta \alpha_F \\ \delta \alpha_B \end{bmatrix}^T \leq \begin{bmatrix} 80 \text{rad/s} \\ 80 \text{rad/s} \\ 7.5 \text{deg} \\ 7.5 \text{deg} \\ 80 \text{rad/s} \\ 80 \text{rad/s} \\ 7.5 \text{deg} \\ 7.5 \text{deg} \end{bmatrix} \quad (14)$$

Provided the PWA representation of the hybrid systems as in (12) and (13) and the constraints as given in (14) a hybrid predictive controller is computed following the approach of multi-parametrically computed constrained receding horizon controllers for hybrid systems [2, 9, 10]. Utilizing a quadratic norm as a metric of optimality, the hybrid MPC consists of computing the optimal control sequence $\mathbf{U}_m^N = [u_m(0), \dots, u_m(N-1)]$ that minimizes the following quadratic control function:

$$\mathbf{J}(x_0, U^N) = \min_{U^N} \{ \mathbf{x}_N^T \mathbf{P}_{M \times M} \mathbf{x}_N + \sum_{k=0}^{N-1} \mathbf{x}_k^T \mathbf{Q}_{M \times M} \mathbf{x}_k^T + \mathbf{u}_k^T \mathbf{R}_{L \times L} \mathbf{u}_k \} \quad (15)$$

$$\begin{aligned} \text{s.t.} \quad & \mathbf{x}(k+1) = \mathbf{A}_{i(k)} \mathbf{x}(k) + \mathbf{B}_{i(k)} \mathbf{u}(k) + \mathbf{f}_{i(k)}, \\ & \mathbf{y}(k) = \mathbf{C}_{i(k)} \mathbf{x}(k) + \mathbf{D}_{i(k)} \mathbf{u}(k), \\ & \mathbf{H}_{i(k)} \mathbf{x}(k) + \mathbf{J}_{i(k)} \mathbf{u}(k) \leq \mathbf{K}_{i(k)} \\ & \mathbf{H}_{i(k)} \mathbf{x}(k) + \mathbf{J}_{i(k)} \mathbf{u}(k) < \mathbf{K}_{i(k)} \\ & \mathbf{x}_N \in T_{set} \end{aligned} \quad (16)$$

where N is the prediction horizon, $\mathbf{P}_{M \times M} \succeq \mathbf{0}$ ($M = 5$), $\mathbf{Q}_{M \times M} \succeq \mathbf{0}$, $\mathbf{R}_{L \times L} \succeq \mathbf{0}$ ($L = 5$) are the weighting matrices of the terminal state, of the states and the manipulated variables respectively, and T_{set} is the terminal set which is computed as the LQR terminal set to guarantee stability properties. The proposed control strategy: a) provides guaranteed global stability of the hybrid model [2, 9] and b) optimal performance in the quadratic sense, while c) respects the incorporated

system constraints. The computation of this controller was done using the Multi-Parametric Toolbox [9].

It is highlighted that the correct transition between the different flight modes is critical for the system safety. As is intuitively understood, if the forward velocity is low, then a complete rotation of the servo angles from helicopter-mode (HM) to fixed-wing mode (FWM) can cause significant altitude loss or even crash. Despite the fact that ideally this issue is handled by the predictive controller, it is possible that the actual vehicle response is disturbed. Accordingly, an additional constraint has been added to the controller and is part of the optimization process. The formulation of this safety constraint is as follows:

$$\text{IF } u \leq 4 \text{m/s THEN } \alpha^r \leq 30^\circ \quad [HM \rightarrow FWM] \quad (17)$$

This logical constraint guarantees that the system will not continue its transition to fixed wing mode as long as the forward velocity is too small hence risking its capability to remain airborne. Such logical constraints can be implemented within the optimization process using the MPT [9].

Finally, it should be mentioned that the proposed controller exceeds the functionality of transition control between the fixed-wing mode and the helicopter mode. It is actually capable of handling the transition between every possible operating point. Of particular interest are operating points that are close to helicopter-mode but have the rotors slightly tilted. Such a mode of flight dynamics can be controlled with a control strategy similar to that of helicopter-mode, while also providing a significant forward force and therefore superior accelerating capabilities.

V. SIMULATION STUDIES

As mentioned, the proposed control strategy is able to handle the mode transition between any of the PWA systems modeled in Section III. Three control tests were performed and are presented within this Section, namely the transition from helicopter to fixed-wing mode, the inverse problem as well as the transition from helicopter mode to a mode close to helicopter mode but with a servo-angle tilted at 15 degrees angle so that a significant acceleration component aids the forward motion of the system. In all cases the complete nonlinear model was used as the control problem plant. The prediction horizon was set to $N = 4$.

Figure 7 depicts the state responses, control actions and controller-PWA system switching of the hybrid modes during the transition from helicopter to fixed-wing mode. As shown, the closed-loop system effectively transits without significant errors or overshoots on the critical off-axis states of altitude velocity and attitude orientation.

Subsequently, the capabilities of the control strategy to stable convert the system from fixed-wing mode to helicopter-mode with minimum oscillations was tested. Figure 8 presents the derived results where the high efficiency is shown. It should be noted that the same controller is used for both transitions, hence, a trade-off is required in the penalty matrices tuning.

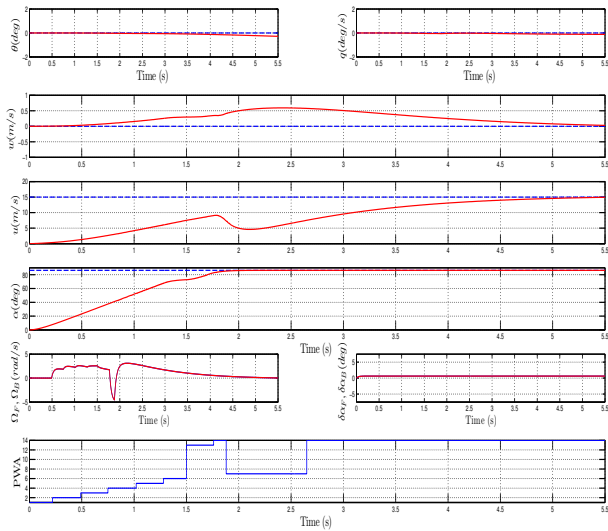


Fig. 7. Helicopter to Fixed-Wing Mode transition controlled response. The last subplot depicts the switching among the different PWA modes as the response evolves over time.

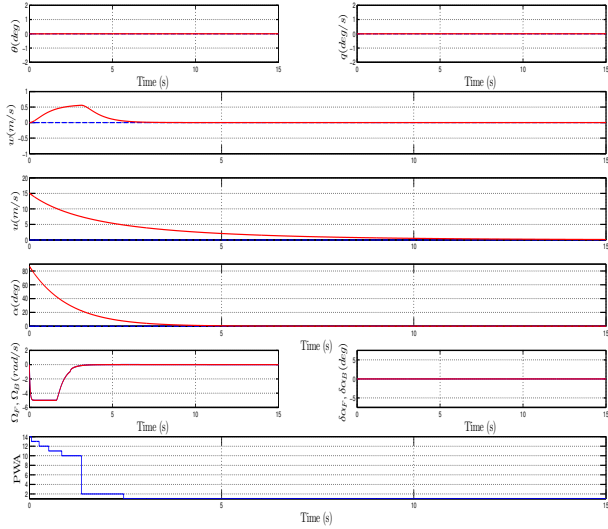


Fig. 8. Fixed-Wing to Helicopter Mode transition controlled response

Finally, Figure 9 depicts the response of the system in the case of mode transition between a system with low velocity and vertical rotors (helicopter-mode) to a mode with rotors tilted at 15 degrees which adds a significant forward motion force component. Such a mode transition is thought to be of great usability for paths that are not so short to be covered in helicopter-mode but also not so long to be covered in fixed-wing mode.

Overall, it was shown that the proposed hybrid-MPC provides an efficient strategy to handle the flight-mode transition problem of Quad-TiltRotors between the extreme cases of helicopter-like and fixed wing-like flying modes as well as between modes that are close in the aforementioned cases which is also useful in order to fully exploit the capabilities of such UAV configurations.

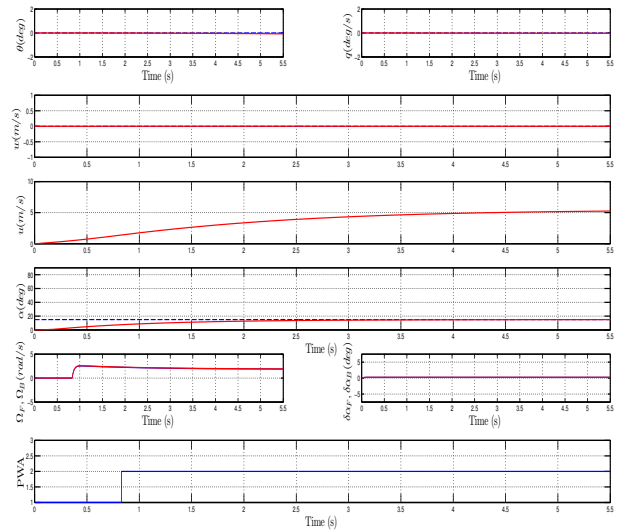


Fig. 9. Transition from mode with $\alpha = u = 0$ to modes with $\alpha = 15$ degrees. No forward velocity reference is tracked here: the vehicle accelerates as long as the airfoil drag does not compensate the forward force component due to the tilted rotors.

VI. CONCLUSIONS

The nonlinear model dynamics of a Quad-TiltRotor UAV type were extracted, and a piecewise affine approximation of the multi-mode flight envelope was developed. Using this representation, a model predictive-based control scheme, and a hybrid systems modeling approach, an innovative flight-mode conversion controller was implemented. The effectiveness of the proposed controller in: a) tackling the complexity of the conversion task, as well as b) the additional capability for exploitation of intermediate flight envelope configurations, were demonstrated via simulation studies.

REFERENCES

- [1] G. N. K. Alexis, C. Papachristos and A. Tzes, "Model predictive quadrotor indoor position control," in *Proceedings of the 19th Mediterranean Control Conference*, Corfu, Greece, 2011, pp. 1247–1252.
- [2] M. Baotic, "Optimal control of piecewise affine systems," Ph.D. dissertation, Swiss Federal Institute of Technology Zurich, 2005.
- [3] Brian L. Stevens and Frank L. Lewis, *Aircraft Control and Simulation*. Wiley Interscience, 1992.
- [4] The MathWorks Inc., *Aerospace Blockset 3 User's Guide*, 2009.
- [5] M. Drela, "XFOIL Subsonic Airfoil Development System," <http://web.mit.edu/drela/Public/web/xfoil/>, 2008.
- [6] C. Papachristos, K. Alexis, and A. Tzes, "Towards a high-end unmanned tri-tiltrotor: Design, modeling and hover control," in *Control Automation (MED), 2012 20th Mediterranean Conference on*, July 2012, pp. 1579–1584.
- [7] G. Flores, J. Escareno, R. Lozano, and S. Salazar, "Quad-tilting rotor convertible mav: Modeling and real-time hover flight control," *Journal of Intelligent & Robotic Systems*, vol. 65, pp. 457–471, 2012.
- [8] R. Naldi and L. Marconi, "Optimal transition maneuvers for a class of v/stol aircraft," *Automatica*, vol. 47, no. 5, pp. 870 – 879, 2011.
- [9] M. Kvasnica, P. Grieder, M. Baotic, and M. Morari, *Multi-Parametric Toolbox (MPT)*, Automatic Control Laboratory, Swiss Federal Institute of Technology (ETH), 2004.
- [10] K. Alexis, G. Nikolakopoulos, and A. Tzes, "Design and experimental verification of a constrained finite time optimal control scheme for the attitude control of a quadrotor helicopter subject to wind gusts," in *2010 International Conference on Robotics and Automation*, Anchorage, Alaska, USA, 2010, pp. 1636–1641.